Supplement of Atmos. Chem. Phys., 25, 6975–6990, 2025
https://doi.org/10.5194/acp-25-6975-2025-supplement

Atmospheric Chemistry and Physics
Open Access

Supplement of

Significant contributions of biomass burning to $PM_{2.5}$-bound aromatic compounds: insights from field observations and quantum chemical calculations

Yanqin Ren et al.

Correspondence to: Haijie Zhang (zhanghaijie@craes.org.cn), Yuanyuan Ji (ji.yuanyuan@craes.org.cn), and Gehui Wang (ghwang@geo.ecnu.edu.cn)

Table S1 Limit of detection (LOD) and concentration in the blank sample of the target compounds in this study.

Compounds	m/z[a]	Vapor Pressure [b] (Pa, 298K)	Molecular structure	LOD (ng μL^{-1})	Concentration in the blank sample (ng m^{-3})
PAHs					
Fluoranthene (Flu)	202	1.2×10^{-3}	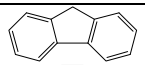	0.0035	NA[c]
Pyrene (Pyr)	202	6.0×10^{-4}	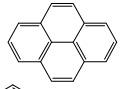	0.0080	NA[c]
benz(*a*)anthracene (BaA)	228	2.8×10^{-5}	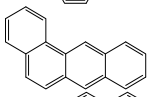	0.0033	NA[c]
chrysene (Chr)	228	8.2×10^{-7}	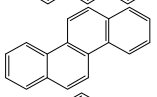	0.0034	NA[c]
benzo(*b*)fluoranthene (BbF)	252	NA[c]	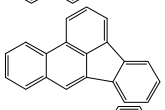	0.0055	NA[c]
benzo(*k*)fluoranthene (BkF)	252	1.3×10^{-7}	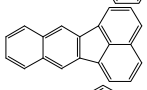	0.0029	NA[c]
benzo(*e*)pyrene (BeP)	252	7.6×10^{-7}	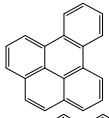	ND[d]	NA[c]
benzo(*a*)pyrene (BaP)	252	7.3×10^{-7}	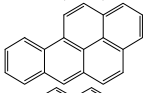	0.0038	NA[c]
Perylene (Per)	252	6.7×10^{-8}	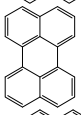	ND[d]	NA[c]
indeno(1,2,3-*cd*)pyrene (IP)	276	NA[c]	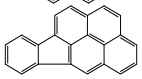	0.0029	NA[c]

benzo(*ghi*)perylene (BghiP)	276	1.3×10^{-8}	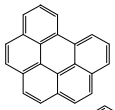	0.0030	NA[c]
dibenz(*a,h*)anthracene (DBA)	278	1.3×10^{-7}	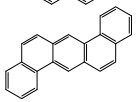	0.0052	NA[c]
coronene	300	NA[c]		ND[d]	NA[c]
OPAHs					
1-naphthaldehyde (1-NapA)	156	NA[c]		ND[d]	NA[c]
9-fluorenone (9-FO)	180	NA[c]	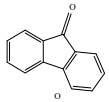	0.0073	NA[c]
anthraquinone (ATQ)	208	1.5×10^{-5}	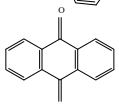	0.013	NA[c]
benzathrone (BZA)	230	NA[c]	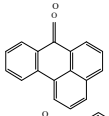	0.012	NA[c]
benzo(a)anthracene-7,12-dione (7,12-BaAQ)	258	NA[c]	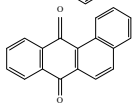	0.022	NA[c]
1,4-chrysenequione (1,4-CQ)	258	NA[c]	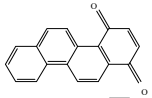	0.37	NA[c]
5,12-naphthacenequione (5,12-NAQ)	258	NA[c]	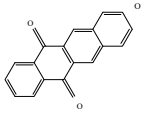	0.040	NA[c]

6H-benzo(cd)pyrene-6-one (BPYRone)	254	NA[c]	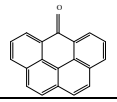	0.019	NA[c]
NPs					
4-nitrophenol (4NP)	196	6.7×10^{-2}	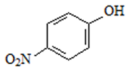	0.00041	NA[c]
3-methyl-4-nitrophenol (3M4NP)	210	NA[c]	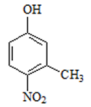	0.00011	NA[c]
4-nitroguaiacol (4NGA)	211	NA[c]	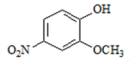	0.0014	NA[c]
5-nitroguaiacol (5NGA)	211	NA[c]	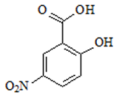	0.0012	NA[c]
4-nitrocatechol (4NC)	284	NA[c]	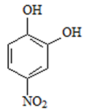	0.0069	NA[c]
2,4-dinitrophenol (2,4-DNP)	241	NA[c]	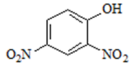	0.0068	NA[c]
4-methyl-5-nitrocatechol (4M5NC)	313	NA[c]	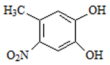	0.00023	NA[c]
3-nitrosalicylic acid (3NSA)	312	NA[c]	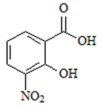	0.00034	NA[c]
3-nitrosalicylic acid (5NSA)	312	NA[c]	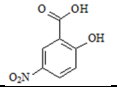	0.00026	NA[c]

[a] Mass-to-charge ratio of fragment ions for qualification and quantification.
[b] The values come from PubChem.
[c] NA: not available.
[d] ND: not detected, because the standards are not commercially available.

Text S1: PMF operation process

To further analyze the quantitative and qualitative effects of primary emissions as well as secondary formation, we applied the Positive Matrix Factorization (PMF) (EPA PMF 5.0 version) receptor model. Daily measurements of SO_2, NO, O_3, $PM_{2.5}$, OC, EC, SO_4^{2-}, NO_3^-, NH_4^+, Na^+, Cl^-, K^+, levoglucosan (Lev.), PAHs, OPAHs, and NPs were used as input data. According to the results of the simulation, the categories of EC and Na^+ were found to be bad. Numerous runs of the model using three to six factors and different combinations of the absorption and concentration data set were carried out. The agreement between the model fit and the correlation between estimated and measured concentrations are respectively depicted by the values of Q and r^2, and the choice of proper factor number for modeling relies on these values (Comero et al., 2009). **Table S2** gives the outcome of Q robust, average r^2, and Q true value. With the dQ value under 5% of the Base Run Q (robust), the Fpeak results were acceptable. Moreover, there is a reasonable physical interpretation of all factors via the evaluation of the variation in maximum individual column standard deviation parameters and the maximum individual column mean since they demonstrated a notable drop with the change in the number of factors in this study (Cesari et al., 2017). All these results indicated the number of factors (four factors) was appropriate (**Fig. S1**).

References

Cesari, D., Benedetto, G. E. D., Bonasoni, P., Busetto, M., and Contini, D.: Seasonal variability of PM2.5 and PM10 composition and sources in an urban background site in Southern Italy, Sci. Total. Environ., 612, 202, 2017.

Comero, S., Capitani, L., and Gawlik, B.: Positive Matrix Factorisation (PMF)–An introduction to the chemometric evaluation of environmental monitoring data using PMF, Office for Official Publications of the European Communities, Luxembourg, 59, 10.2788/2497, 2009.

Table S2 Values of *Q* (robust), *Q* (true) and average r^2 for the modeling results in the whole campaign.

species	the whole sampling period
Q (robust)	4071.55
Q (true)	4834.02
SO_2 (r^2)	0.93
NO (r^2)	0.98
O_3 (r^2)	0.82
$PM_{2.5}$(r^2)	0.92
OC(r^2)	0.84
SO_4^{2-}(r^2)	0.83
NO_3^-(r^2)	0.93
NH_4^+(r^2)	0.97
Cl^-(r^2)	0.58
K^+(r^2)	0.55
Levoglucosan (r^2)	0.91
PAHs(r^2)	0.92
OPAHs(r^2)	0.67
NPs(r^2)	0.45

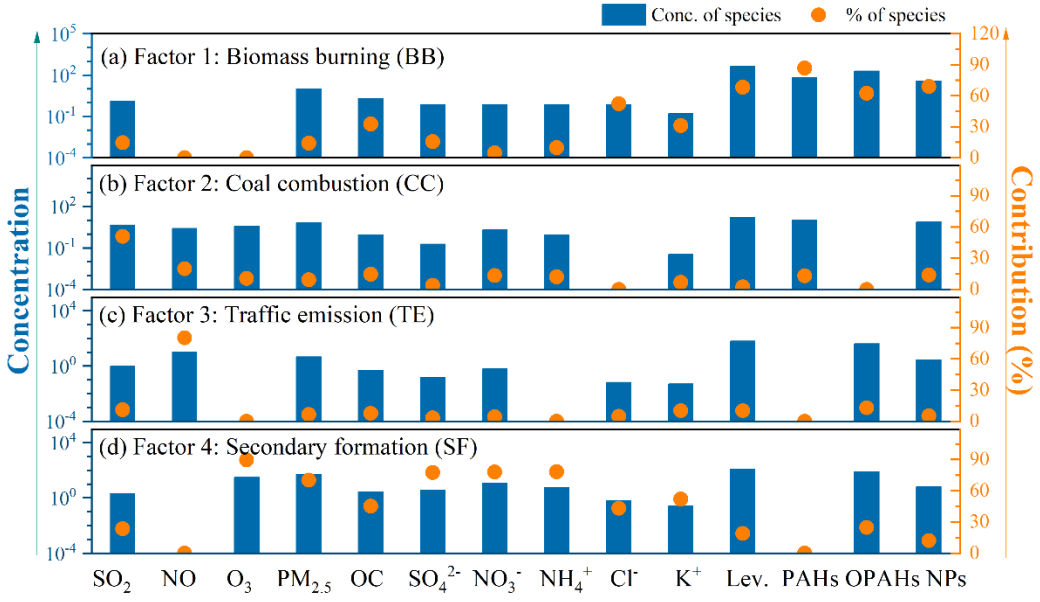

Fig.S1 Source profiles of aromatic compounds obtained from PMF analysis (lev. – levoglucosan, and NPs – nitrated phenols).

Table S3 Diagnostic ratios of PAHs used as source indicator.

Ratios	Dongying			Sources			
	The whole campaign	Before heating	During heating	Gasoline-engines	Diesel-engines	Coal combustion	Biomass and coal burning
IP/BghiP	1.07	1.03	1.09	0.22[a]	0.50[a]	1.3[a]	
BghiP/BeP	0.7	0.68	0.71	2.0[b]		0.8[b]	

[a] Data from (Grimmer et al., 1983).
[b] Data from (Ohura et al., 2004).

References

Grimmer, G., Jacob, J., and Noujack, K. W.: Profile of the polycyclic aromatic hydrocarbons from lubricating oils inventory by GCGC/MS-PAH in environmental materials, Part 1, Fresenius Zeitschrift fur Analytishe Chemie, 314, 13–19, 1983.

Ohura, T., Amagai, T., Fusaya, M., and Matsushita, H.: Polycyclic aromatic hydrocarbons in indoor and outdoor environments and factors affecting their concentrations, Environ. Sci. Technol., 38, 77–83, 2004.

Table S4. The electronic energy E_{DFT} and the Gibbs free energy G_{DFT} of reactant monomers at the M062X/6-311++G(3df,3pd) level of theory. All energies are in Hartree and T = 298 K.

Phase	Monomers	E_{DFT}	G_{DFT}
gas phase	OH	-75.72917436	-75.737513
	NO_2	-205.0652725	-205.079389
	H_2O	-76.42489661	-76.42151
	Nitrobenzene	-436.7193104	-436.64666
	Phenol	-307.4438958	-307.367152
	cis-HONO	-205.6987083	-205.701639
	p-Cresol	-346.7471095	-346.645291
	IM1	-306.7561086	-306.693032
	IM2	-436.0322146	-435.973217
	IM3	-346.065347	-345.97788
	IM4	-421.9825728	-421.878094
	IM5	-421.2955673	-421.203709
	4NP	-511.9504536	-511.874497
	4M5NC	-626.485922	-626.380532
liquid phase	NO_2	-205.0667262	-205.080949
	Phenol	-307.4507633	-307.374249
	IM1	-306.7629835	-306.700134
	IM4	-421.9910599	-421.88603
	IM5	-421.3038828	-421.212406

Table S5. The electronic energy E_{DFT}, Gibbs free energy G_{DFT} and the imaginary frequency of TS calculated for the formation of 4NP by Phenol at the M06-2X/6-311++G(3df,3pd) level of theory. All energies are in Hartree and T = 298 K.

phase	Steps	Molecules	E_{DFT}	G_{DFT}	ν_{im} (cm^{-1})
gas phase	H-abstraction by OH	$RC_{ph\text{-}OH}$	-383.1814862	-383.099624	
		$TS_{ph\text{-}OH}$	-383.1635205	-383.085864	-1237.1969*i*
		IM1---H_2O	-383.1866979	-383.106300	
	H-abstraction by NO_2	$RC_{ph\text{-}NO2}$	-512.5131701	-512.435702	
		$TS_{ph\text{-}NO2}$	-512.4535054	-512.382309	-1585.4851*i*
		IM1---cis-HONO	-512.4624726	-512.388355	
	NO_2 addition	IM1+NO_2	-511.8213812	-511.772421	
		4NP	-511.9504536	-511.874497	
liquid phase	H-abstraction by NO_2	$RC_{ph\text{-}NO2}$	-512.5192961	-512.444301	
		$TS_{ph\text{-}NO2}$	-512.4621090	-512.390595	-1628.5336*i*
		IM1---cis-HONO	-512.4713810	-512.397119	
	NO_2 addition	IM1+NO_2	-511.8297097	-511.781083	
		4NP	-511.9625041	-511.886975	

Table S6. The electronic energy E_{DFT}, Gibbs free energy G_{DFT} and the imaginary frequency of TS calculated for the formation of 4NP by Nitrobenzene at the M06-2X/6-311++G(3df,3pd) level of theory. All energies are in Hartree and T = 298 K.

phase	Steps	Molecules	E_{DFT}	G_{DFT}	ν_{im} (cm^{-1})
gas phase	H-abstraction by OH	$RC_{Nb\text{-}OH}$	-512.4506363	-512.375738	
		$TS_{Nb\text{-}OH}$	-512.4374359	-512.364003	-1412.9321*i*
		IM2---H_2O	-512.4617599	-512.385901	
	OH addition	IM2+OH	-511.7613890	-511.710730	
		4NP	-511.9382659	-511.862064	

Table S7. The electronic energy E_{DFT}, the Gibbs free energy G_{DFT} and the imaginary frequency of TS calculated for the formation of 4M5NC by *P*-Cresol at the M06-2X/6-311++G(3df,3pd) level of theory. All energies are in Hartree and T = 298 K.

Steps	phase	Molecules	E_{DFT}	G_{DFT}	ν_{im} (cm^{-1})
Step 1: H-abstraction by OH	gas phase	$RC_{pC\text{-}OH}$	-422.4918755	-422.383209	
		$TS_{pC\text{-}OH}$	-422.4773183	-422.371344	-1188.6897*i*
		IM3---H_2O	-422.5033608	-422.395347	
Step 2: OH addition	gas phase	IM3+OH	-421.7945214	-421.715393	
		IM4	-421.9825728	-421.878094	
Step 3: H-abstraction by OH	gas phase	IM4---OH	-497.7235822	-497.612110	
		TS_{OH}	-497.7035890	-497.596750	-1196.772*i*
		IM5---H2O	-497.7267084	-497.618336	
Step 3: H-abstraction by NO_2	gas phase	IM4---NO_2	-627.0553941	-626.950478	
		TS_{NO2}	-626.9941024	-626.892971	-1555.5559*i*
		IM5---HONO	-627.0054168	-626.899673	
Step 3: H-abstraction by NO_2	liquid phase	IM4---NO_2	-627.0642238	-626.958635	
		TS_{NO2}	-627.0043629	-626.903942	-1613.0626*i*
		IM5---HONO	-627.0130492	-626.908874	
Step 4: NO_2 addition	gas phase	IM5+NO_2	-626.3608398	-626.283098	
		4M5NC	-626.485922	-626.380532	
Step 4: NO_2 addition	liquid phase	IM5+NO_2	-626.370609	-626.293355	
		4M5NC	-626.4995951	-626.394496	

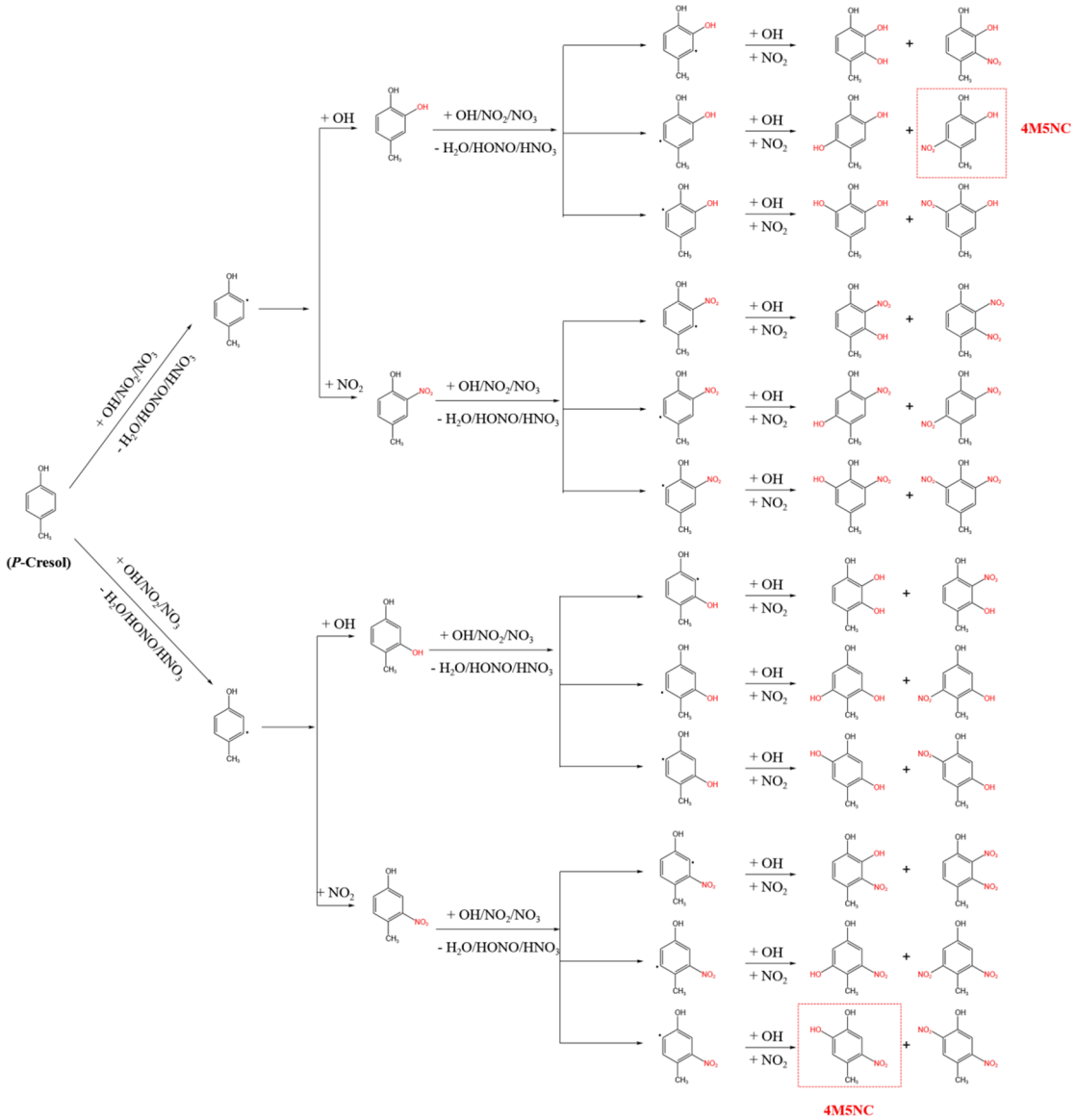

Fig.S2 Potential reaction mechanism of *P*-Cresol with OH, NO_2 or NO_3 at the M06-2X/6-311++G(2df,2p) level of theory.